

Improving Graph Neural Network Training, Defense, Hypergraph Partitioning and Spectral Clustering via Adversarial Robustness Evaluation

Yongyu Wang

Abstract. Graph Neural Networks (GNNs) are a highly effective neural network architecture for processing graph-structured data. Unlike traditional neural networks that rely solely on the features of the data as input, GNNs leverage both the graph structure, which represents the relationships between data points, and the feature matrix of the data to optimize their feature representation. This unique capability enables GNNs to achieve superior performance across various tasks. However, it also makes GNNs more susceptible to noise from both the graph structure and data features, which can significantly increase the training difficulty and degrade their performance. To address this issue, this paper proposes a novel method for selecting noise-sensitive training samples from the original training set to construct a smaller yet more effective training set for model training. These samples are used to help improve the model’s ability to correctly process data in noisy environments. We have evaluated our approach on three of the most classical GNN models—GCN, GAT, and GraphSAGE—as well as three widely used benchmark datasets: Cora, Citeseer, and PubMed. Our experiments demonstrate that the proposed method can substantially boost the training of Graph Neural Networks compared to using randomly sampled training sets of the same size from the original training set and the larger original full training set. We further proposed a robust-node based hypergraph partitioning method, an adversarial robustness based graph pruning method for GNN defenses, a robust spectral clustering method and a related spectral edge attack method.

1 Introduction

The rise of Graph Neural Networks (GNNs) has brought about a transformative shift in the field of machine learning, particularly for tasks involving graph-structured data [1–4]. These networks have demonstrated success across a wide array of real-world scenarios, including recommendation systems [5], traffic forecasting [6], chip design [7], language processing [8] and social network analytics [9]. The unique advantage of GNNs lies in their ability to effectively leverage the graph that represents the relationships between data points to optimize their feature representations. This enables GNNs to fully utilize the crucial graph topology inherent in graph-structured data, unlike traditional neural networks,

Correspondence to: yongyuw@mtu.edu

which optimize data representations based solely on feature vectors, thus overlooking the valuable graph structure.

However, like other neural networks, GNNs are susceptible to noise in the feature space [10,11]. Additionally, the introduction of graph structure introduces another layer of interference, as GNNs are also affected by noise within the graph itself. Research has shown that even slight modifications to the graph—such as adding, removing, or rearranging a small number of edges—can significantly impact the performance of GNNs [12,13].

The feature vectors contaminated by noise, along with erroneous and redundant edges in the graph topology, can be viewed as adversarial attacks that mislead the GNNs. To address this issue, researchers have proposed various methods to reduce the impact of noise on the model’s performance. These approaches can be divided into two categories: reactive and proactive defenses. Reactive defenses focus on identifying adversarial examples within the model’s inputs, as explored in previous studies [14–16]. On the other hand, proactive defenses aim to strengthen the model’s robustness, making it less susceptible to adversarial attacks, as demonstrated by methods proposed in works such as [17,18].

However, due to the diversity of noise types and model structures, developing effective methods to defend against noise across various scenarios remains a significant challenge. Unlike existing approaches that focus on mitigating the effects of noise, we argue that, given the inevitability of noise, the focus should shift toward how to better leverage it. From this new perspective, this paper proposes a framework that first identifies the most noise-sensitive training samples and then uses these samples to construct a smaller but more effective training set for training the GNN model. This approach enhances the model’s ability to correctly process noisy data.

We evaluated our proposed training method using three classical GNN models—GCN [1], GAT [2], and GraphSAGE [19]—on three widely used benchmark datasets for GNN performance evaluation: Cora, Citeseer, and PubMed. The experimental results demonstrate that our method achieves the best training performance compared to two other approaches: a training set of the same size constructed by random sampling from the original full training set, and the larger original full training set.

In the end of the paper, we also provide a robust-node based hypergraph partitioning method, an adversarial robustness based graph pruning method for GNN defenses, a robust spectral clustering method and a related spectral edge attack method.

2 Preliminaries

2.1 The Vulnerability of GNNs to Noise

The vulnerability of Graph Neural Networks (GNNs) to noise refers to the difficulty GNNs face in maintaining consistent outputs when exposed to perturbations in the graph structure, such as the presence of incorrect or redundant

edges in the input graph, or errors in the feature representations within the input feature matrix. [23] investigated the task- and model-agnostic vulnerabilities of GNNs, showing that these networks are very vulnerable to adversarial perturbations, regardless of the downstream task.

2.2 Spectral Graph Theory

Spectral Graph Theory is a mathematical method that uses the eigenvalues and eigenvectors of the Laplacian matrix of a graph to study its properties. Given a graph $G = (V, E, w)$, where V represents the set of vertices, E is the set of edges, and w is a function assigning positive weights to each edge. The Laplacian matrix of graph G , which is a symmetric diagonally dominant (SDD) matrix, is defined as follows:

$$L(p, q) = \begin{cases} -w(p, q) & \text{if } (p, q) \in E, \\ \sum_{(p,t) \in E} w(p, t) & \text{if } p = q, \\ 0 & \text{otherwise.} \end{cases} \quad (1)$$

For better numerical stability and to make the Laplacian matrix scale-invariant, the normalized Laplacian matrix L_{norm} can be computed as:

$$L_{\text{norm}} = D^{-1/2} L D^{-1/2}$$

According to spectral graph theory, analyzing a graph often requires only one or a few specific eigenvalues and their corresponding eigenvectors [20]. For example, when analyzing the clustering structure of a graph using spectral graph theory, only the smallest eigenvalues and their corresponding eigenvectors are useful [21]. Therefore, for a Laplacian matrix, it is unnecessary to compute all the eigenpairs through direct eigen decomposition, and for a large-scale graph, the computational cost would be too high. The Courant-Fischer Minimax Theorem [22] allows the eigenvalues to be computed iteratively without explicitly calculating all the eigenvalues. Specifically:

The k -th largest eigenvalue of the Laplacian matrix $L \in \mathbb{R}^{|V| \times |V|}$ can be computed as follows:

$$\lambda_k(L) = \min_{\dim(U)=k} \max_{x \in U, x \neq 0} \frac{x^T L x}{x^T x}$$

In many practical applications, the problem-solving process involves not just a single matrix, but rather the relationship between two matrices. Therefore, the Courant-Fischer Minimax Theorem is extended to the generalized case, resulting in the following Generalized Courant-Fischer Minimax Theorem:

Consider two Laplacian matrices $L_X \in \mathbb{R}^{|V| \times |V|}$ and $L_Y \in \mathbb{R}^{|V| \times |V|}$, where it holds that $\text{null}(L_Y) \subseteq \text{null}(L_X)$. Under the condition $1 \leq k \leq \text{rank}(L_Y)$, the k -th largest eigenvalue of the matrix $L_Y^+ L_X$ can be computed as follows:

$$\lambda_k(L_Y^+ L_X) = \min_{\dim(U)=k, U \perp \text{null}(L_Y)} \max_{x \in U} \frac{x^T L_X x}{x^T L_Y x}$$

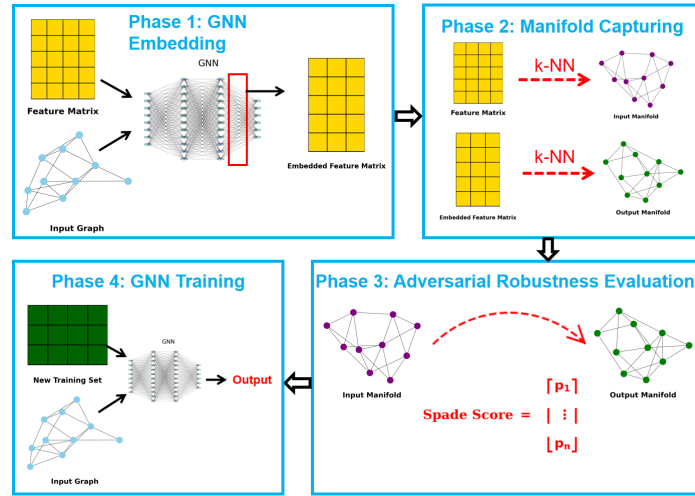


Fig. 1: Overview of the proposed method.

3 Method

Figure 1 shows the proposed method for training GNNs using top non-robust training samples in the training set, which consists of four key phases: Phase (1) is GNN embedding, which uses the original input to train a GNN and takes the output of the hidden layer as the embedding result of the data’s feature matrix; In Phase (2), we use k-NN graphs to capture the underlying manifolds of the input feature matrix and the embedded feature matrix; In Phase (3), we calculate each node’s level of non-robustness using the input manifold and the output manifold; In Phase (4), we use the top non-robust samples selected from the training set to train the GNN. In the rest of this section, we provide a detailed description of these four phases.

3.1 Phase 1: GNN Embedding

[24] proposed leveraging a bijective distance mapping between the manifolds of a model’s input and output data to analyze the adversarial robustness of each data point for a given model.

To obtain the output data of the GNN model, we first train the GNN using the original feature matrix and input graph. Once trained, the GNN is then used to transform the input feature matrix. Since the final layer of a GNN is typically task-specific—such as a softmax layer for multi-class classification tasks—we take the output of the hidden layer before the final output layer as the embedding result.

3.2 Phase 2: Manifold Capturing

The manifold of the data is typically captured using graphs, and k-nearest neighbor graphs are the most widely used for this purpose. In this phase, we use k-nearest neighbor (k-NN) graphs to capture the underlying manifolds of the input feature matrix and the embedded feature matrix. The conventional k-NN graph construction algorithm exhibits a time complexity of $O(|N|^2)$, where $|N|$ is the total number of nodes in the graph. Such quadratic complexity makes it impractical for large-scale datasets. To overcome this limitation, an approximate kNN graph construction algorithm can be employed [25]. This approach leverages an extension of the probabilistic skip list structure to achieve a reduced time complexity of $O(|N| \log |N|)$, which is more suitable for large-scale data processing.

3.3 Phase 3: Adversarial Robustness Evaluation

Let L_X and L_Y denote the Laplacian matrices corresponding to the k-NN graphs of the input feature matrix and the embedded feature matrix constructed in phase 2, respectively. Building on the theoretical framework introduced in [24], we leverage the largest generalized eigenvalues and their associated eigenvectors of $L_Y^+ L_X$ to assess the robustness of each individual sample to noise during the processing by a given model. Specifically, we calculate the weighted eigensubspace matrix $V_s \in \mathbb{R}^{|V| \times s}$ to perform spectral embedding of the input manifold $G_X = (V, E_X)$, where $|V|$ represents the total number of nodes. The matrix V_s is expressed as:

$$V_s = [v_1 \sqrt{\zeta_1}, v_2 \sqrt{\zeta_2}, \dots, v_s \sqrt{\zeta_s}],$$

where $\zeta_1 \geq \zeta_2 \geq \dots \geq \zeta_s$ are the top s eigenvalues of $L_Y^+ L_X$, and v_1, v_2, \dots, v_s are the corresponding eigenvectors.

Using V_s , we project the nodes of G_X into an s -dimensional space, representing each node p as the p -th row of V_s . According to [24], the stability of an edge $(p, q) \in E_X$ is quantified by computing the spectral embedding distance between nodes p and q :

$$\|V_s^\top e_{p,q}\|_2^2.$$

To assess the robustness of a node p , a metric referred to as the *Spade score* is defined as the average embedding distance to the neighbors within the input manifold:

$$\text{Spade}(p) = \frac{1}{|N_X(p)|} \sum_{q \in N_X(p)} \|V_s^\top e_{p,q}\|_2^2,$$

where $N_X(p)$ represents the set of neighbors of node p in G_X . A higher $\text{Spade}(p)$ value suggests that node p is more prone to adversarial attacks.

3.4 Phase 4: GNN Training

For the samples in the training set, we rank them in descending order based on their Spade scores and select the top portion to form a new, smaller training

set. The points in this new training set are those that are highly susceptible to noise and likely to mislead the GNN. By training the GNN using only these noise-sensitive samples, we are effectively enhancing the GNN’s ability to resist being misled by such samples.

4 Experiments

We have evaluated our framework on three of the most popular GNN models and three classic benchmark datasets.

4.1 Experimental Setup

Data Sets We evaluate the proposed method on three standard citation network benchmarks, where nodes represent documents, edges correspond to citations, and each node is associated with a sparse bag-of-words feature vector and a class label. The key statistics of these datasets are summarized in Table 1.

- **Cora**: A dataset of scientific publications categorized into seven classes.
- **Citeseer**: A dataset of scientific publications that is sparser than Cora and exhibits a more uneven class distribution, making it more challenging for graph-based classification methods.
- **PubMed**: A large biomedical dataset where nodes are represented by TF-IDF word vectors from a 500-word vocabulary.

Table 1: Statistics of datasets used in our experiments.

Dataset	Nodes	Edges	Classes	Features
Cora	2,708	5,429	7	1,433
Citeseer	3,327	4,732	6	3,703
PubMed	19,717	44,338	3	500

GNN Models We use the following three commonly used GNN models for our experiments:

- **Graph Convolutional Network (GCN)**: A widely used model that applies convolution-like operations to graph-structured data by aggregating information from neighboring nodes using a layer-wise propagation rule.
- **Graph Attention Network (GAT)**: Introduces an attention mechanism to assign different importance weights to neighboring nodes during the message-passing process.
- **GraphSAGE**: An inductive model that learns aggregation functions to generate node embeddings by sampling and aggregating features from a fixed number of neighboring nodes.

Detailed Model Implementation and Parameter Settings

- **GCN:** We use the same GCN architecture and parameter settings for all three datasets. The model consists of two graph convolutional layers: the first layer transforms node features to a 64-dimensional space, and the second layer maps them to the number of output classes, with ReLU activation applied after the first convolution. For the Cora dataset, the learning rate is set to 0.01. For the Citeseer and PubMed datasets, it is set to 0.1.
- **GAT:** For the Cora dataset, the GAT model consists of two layers: the first layer has 4 attention heads with 8 hidden units each, followed by an ELU activation, and the second layer has 1 attention head that outputs the number of class logits. For the Citeseer dataset, the GAT model also has two layers: the first layer uses 8 attention heads with 8 hidden units each, followed by an ELU activation, and the second layer has 1 attention head that outputs the class logits. For the PubMed dataset, the GAT model has the same structure as the Citeseer model but includes layer normalization after each layer and uses a Leaky ReLU activation after the first layer. For the Cora dataset, the learning rate is set to 0.01. For the Citeseer dataset, it is set to 0.1, and for the PubMed dataset, it is set to 0.05.
- **GraphSAGE:** The GraphSAGE architecture for the Cora and Citeseer datasets consists of two layers: the first layer uses **SAGEConv** with 64 hidden units, followed by batch normalization, ReLU activation, and a dropout layer with a probability of 0.5. The second layer uses **SAGEConv** with 64 input features and outputs the class labels. The architecture for the PubMed dataset also consists of two layers, but the first layer uses **SAGEConv** with 32 hidden units, followed by batch normalization, ReLU activation, and a dropout layer. The second layer uses **SAGEConv** with 32 input features and outputs the class labels. For all three datasets, the learning rate is set to 0.05.

For all the experiments, the Adam optimizer is used with a weight decay of 5×10^{-4} , and the loss function for multi-class classification is CrossEntropyLoss. The number of eigenvectors is set to 10, and the value of k in k-NN is set to 20.

4.2 Results

We first perform an 80-20 split of the entire dataset by randomly sampling 80% of the samples to form the original full training set and using the remaining 20% as the test set. Then, we construct two different types of training sets: (1) forming the training set by selecting the top 80% of non-robust samples from the original full training set using our method; (2) forming the training set by randomly sampling 80% of the original full training set.

We train the GNN models using the original full training set and the two smaller training sets mentioned above, and the classification accuracy across different epochs is shown in Table 2. In these charts, **Random** represents the training set constructed by randomly sampling 80% of the original full training

set, **Ours** represents the training set constructed using our method, and **Full** represents the original full training set.

From the experimental results, it can be observed that in all 9 combinations of the three GNN models and the three datasets, the training set constructed using our method achieved the highest classification accuracy after 5 epochs of training. Moreover, the advantage of our method is particularly evident on the largest dataset, PubMed. On PubMed, our method outperforms the second-best method by **14.1%**, **7.4%**, and **3.4%** in accuracy for the GCN, GAT, and GraphSAGE models, respectively.

Our method not only significantly outperforms the randomly sampled training sets of the same size but also demonstrates substantial advantages compared to the full training sets, which are 20% larger, highlighting the effectiveness of our approach. The experimental results further show that randomly selecting 80% of the training samples from the full training set yields almost no difference in performance compared to using the full set. However, when 80% of the samples are selected using our method, which prioritizes the most non-robust nodes, the training performance is significantly improved. This demonstrates that focusing on non-robust samples during training, rather than uniformly sampling all nodes, enables the model to better adapt to unavoidable noise, resulting in superior performance on the test set.

5 Improving Hypergraph partitioning

Our method is built on the key idea of treating nodes that are robust to perturbations separately from those that are vulnerable. For nodes that are less susceptible to noise and adversarial interference, we directly apply a hypergraph partitioning algorithm to obtain their partitions. In contrast, for nodes that are more easily affected by such perturbations, we do not rely on hypergraph spectral partitioning; instead, we infer their partition membership based on their relationships with the robust nodes and propagate the partitioning results from the robust subset to these vulnerable nodes. Specifically, the proposed method consists of the following five phases.

5.1 Phase 1: Hypergraph Spectral Embedding

We first perform a spectral embedding of the hypergraph by mapping it into the feature space spanned by the K eigenvectors of its adjacency matrix corresponding to the largest eigenvalue magnitudes.

5.2 Phase 2: Manifold Capturing

Data manifolds are commonly modeled using graphs, with k-nearest neighbor (k-NN) graphs being one of the most prevalent choices. In this stage, we construct a k-NN graph to capture the underlying manifold structure of the spectrally embedded hypergraph. A standard k-NN construction procedure has a

Table 2: Classification Accuracy Across Epochs for GCN, GAT, and GraphSAGE on Cora, Citeseer, and PubMed

Model	Dataset	Training Set	Epoch 1	Epoch 2	Epoch 3	Epoch 4	Epoch 5
GCN	Cora	Random	0.2939	0.3290	0.5360	0.7209	0.7671
		Ours	0.5416	0.6580	0.6525	0.7375	<u>0.8041</u>
		Full	0.2939	0.3290	0.5527	0.7227	<u>0.8041</u>
	Citeseer	Random	0.2331	0.6030	0.6030	0.6256	0.6256
		Ours	0.4797	0.5278	0.5609	0.6316	<u>0.6947</u>
		Full	0.2406	0.5925	0.5925	0.6541	0.6541
	PubMed	Random	0.3918	0.4420	0.5836	0.6191	0.6191
		Ours	0.3974	0.5181	0.7515	0.8052	<u>0.8080</u>
		Full	0.3921	0.4484	0.6082	0.6082	0.6670
GAT	Cora	Random	0.3124	0.3623	0.4603	0.6488	0.7634
		Ours	0.4954	0.6007	0.6506	0.7726	<u>0.8299</u>
		Full	0.3216	0.3604	0.4713	0.6654	0.7782
	Citeseer	Random	0.6451	0.6451	0.6451	0.6917	0.6917
		Ours	0.5594	0.5504	0.6105	0.7053	<u>0.7504</u>
		Full	0.6331	0.6331	0.6617	0.7158	0.7158
	PubMed	Random	0.4027	0.4603	0.5787	0.5787	0.5787
		Ours	0.4174	0.3977	0.4154	0.5580	<u>0.6528</u>
		Full	0.3987	0.4415	0.5455	0.5455	0.5455
GraphSAGE	Cora	Random	0.4824	0.7689	0.7745	0.7893	0.8041
		Ours	0.4991	0.7006	0.7486	0.8115	<u>0.8244</u>
		Full	0.4880	0.7745	0.7837	0.8059	<u>0.8244</u>
	Citeseer	Random	0.4797	0.6737	0.6902	0.7038	0.7113
		Ours	0.4857	0.6451	0.6692	0.7188	<u>0.7624</u>
		Full	0.4812	0.6872	0.6872	0.6992	0.7218
	PubMed	Random	0.3974	0.6429	0.7406	0.7697	0.7735
		Ours	0.3977	0.5945	0.6523	0.7210	<u>0.8078</u>
		Full	0.3974	0.6378	0.7484	0.7652	0.7662

time complexity of $O(|N|^2)$, where $|N|$ denotes the number of nodes, which becomes prohibitive for large-scale datasets. To address this issue, we adopt an approximate k -NN graph construction algorithm [25], which extends a probabilistic skip-list-like structure and reduces the complexity to $O(|N| \log |N|)$, making it far more suitable for large-scale data processing.

5.3 Phase 3: Adversarial Robustness Evaluation

Let L_X and L_Y denote the Laplacian matrices associated with the hypergraph H and the k -NN graph constructed from the spectrally embedded hypergraph in phase 2, respectively. Following the theoretical framework in [24], we exploit the dominant generalized eigenvalues of $L_Y^+ L_X$ and their corresponding eigenvectors to characterize the sensitivity of each sample to noise under a given model. In particular, we compute a weighted eigensubspace matrix $V_s \in \mathbb{R}^{|V| \times s}$ to obtain a spectral embedding of the input manifold $G_X = (V, E_X)$, where $|V|$ is the number of nodes. The matrix V_s is defined as

$$V_s = [v_1 \sqrt{\zeta_1}, v_2 \sqrt{\zeta_2}, \dots, v_s \sqrt{\zeta_s}],$$

where $\zeta_1 \geq \zeta_2 \geq \dots \geq \zeta_s$ are the largest s eigenvalues of $L_Y^+ L_X$, and v_1, v_2, \dots, v_s are the associated eigenvectors.

Using V_s , each node p in G_X is mapped to the p -th row of V_s , yielding an s -dimensional spectral embedding. As described in [24], the stability of an edge $(p, q) \in E_X$ can then be measured by the spectral embedding distance between nodes p and q :

$$\|V_s^\top e_{p,q}\|_2^2.$$

To quantify the robustness of a node p , a score termed the *Spade score* is introduced as the average embedding distance to its neighbors on the input manifold:

$$\text{Spade}(p) = \frac{1}{|N_X(p)|} \sum_{q \in N_X(p)} \|V_s^\top e_{p,q}\|_2^2,$$

where $N_X(p)$ denotes the neighbor set of node p in G_X . A larger value of $\text{Spade}(p)$ indicates that node p is more vulnerable to adversarial perturbations.

5.4 Phase 4: Sub-Hypergraph Partitioning

For the nodes in the hypergraph H , we first rank them in descending order according to their Spade scores and then select the bottom portion to form the node set of a sub-hypergraph. The nodes contained in this sub-hypergraph are those that are highly robust to noise in the hypergraph and to misleading or redundant hyperedges. We then apply a standard hypergraph partitioning algorithm to this sub-hypergraph to obtain the partitioned sub-hypergraph.

5.5 Label Propagation from Robust to Non-Robust Nodes

The nodes that are not included in the robust node set are referred to as non-robust nodes. Since these nodes are vulnerable to adversarial perturbations and attacks that affect hypergraph spectral partitioning, we do not directly apply the hypergraph spectral partitioning algorithm to determine their partitions. Instead, we infer their partition membership based on their relationships with the robust nodes, effectively propagating the partitioning result from the robust subset to the non-robust nodes. Specifically, for each non-robust node, we identify the robust node with which it co-occurs in hyperedges in H most frequently, and assign the non-robust node to the same partition as that robust node.

The complete algorithm of the proposed method has been shown in Algorithm 1.

Algorithm 1 The Algorithm Flow

Input: A hypergraph $H = (V, E)$

Output: Partitioned Hypergraph.

- 1: Extract the adjacency matrix A from the input hypergraph H .
 - 2: Compute the Laplacian matrix \mathbf{L}_H for the graph H .
 - 3: Compute the eigenvectors u_1, \dots, u_k that correspond to the bottom k nonzero eigenvalues of A .
 - 4: Construct $U \in \mathbb{R}^{n \times k}$, with k eigenvectors of A stored as columns.
 - 5: Construct a k -nearest neighbor graph $G = (V, E)$ from U .
 - 6: Compute the Laplacian matrix \mathbf{L}_U for the graph U .
 - 7: Compute the SPADE score of each node.
 - 8: Form a robust node set from nodes with small SPADE scores, while constructing a non-robust node set from nodes with large SPADE scores.
 - 9: Construct a sub-hypergraph S consisting of the robust node set and all hyperedges in H that connect only these robust nodes.
 - 10: For each non-robust node, count the number of hyperedges in H where it appears together with each robust node.
 - 11: Apply standard hypergraph spectral partitioning on S .
 - 12: For each non-robust node, identify the robust node with which it co-occurs in hyperedges in H most frequently, and assign the non-robust node to the partition containing that robust node.
 - 13: Return the partitioned hypergraph.
-

5.6 Experiments

We perform extensive experiments to evaluate the performance of the proposed spectral hypergraph coarsening method on a suite of VLSI-related benchmark datasets, from “ibm01” to “ibm04”. To ensure a fair comparison, we also apply

Datasets are available at: <https://vlscad.ucsd.edu/UCLAWeb/cheese/ispd98.html>.

Table 3: The average local conductance (Φ) comparison between our methods and other methods

Hypergraphs	V	E	Spectral (S)	Spectral (C)	Metis (S)	Metis (C)	Hmetis	HyperSF	Ours
ibm01	12752	14111	0.94	0.81	0.84	0.78	0.65	0.44	0.28
ibm02	19601	19584	0.94	0.84	0.83	0.79	0.69	0.52	0.43
ibm03	23136	27401	0.95	0.86	0.85	0.79	0.67	0.48	0.41
ibm04	27507	31970	0.95	0.84	0.84	0.78	0.68	0.47	0.40

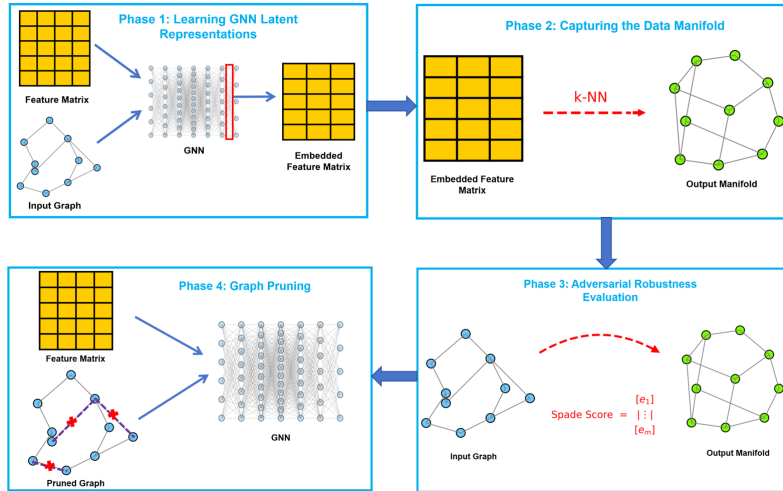


Fig. 2: Overview of the proposed method.

several existing hypergraph coarsening techniques to the same set of benchmarks and compare their results against ours. For brevity, we refer to the star and clique models as S and C, respectively. The experimental results are shown in Table 3. It can be seen that our method consistently outperforms all competing methods across all four datasets.

6 Pruning Graphs by Adversarial Robustness Evaluation to Strengthen GNN Defenses

Figure 2 shows the proposed method for pruning graphs for GNNs, which consists of four key phases: Phase (1) is learning GNN latent representation, We train a GNN and then use the activations of its hidden layer as the embedding of the original feature matrix; In Phase (2), we use k-NN graphs to capture the underlying manifold of the embedded feature matrix; In Phase (3), we calculate each edge’s level of non-robustness using the input graph and the output manifold; In Phase (4), we remove the top non-robust edges from the input graph and

use it as the new input graph for GNNs. In the rest of this section, we provide a detailed description of these four phases.

6.1 Phase 1: Learning GNN Latent Representations

[24] introduced a framework that analyzes the adversarial robustness of individual edges by constructing a bijective distance mapping between the manifolds of a model’s input space and output space.

In our setting, we first train a GNN on the original feature matrix together with the given input graph to obtain a well-fitted model. After training, this GNN is used to map the input features into a latent representation space. Since the last layer of a GNN is typically tailored to the downstream task (for example, a softmax layer in the case of multi-class node classification), we use the activations of the penultimate hidden layer as the embedding of each node, rather than the final task-specific outputs.

6.2 Phase 2: Capturing the Data Manifold

A common way to approximate the underlying data manifold is to represent it with a graph, where nodes correspond to data points and edges reflect local neighborhood relationships. Among such constructions, k -nearest neighbor (k -NN) graphs are particularly popular. In this phase, we construct a k -NN graph on top of the embedded feature matrix obtained from the GNN, so as to model the manifold structure in the latent space.

The standard k -NN graph construction procedure has a time complexity of $O(|N|^2)$, where $|N|$ denotes the number of nodes, which becomes prohibitive for large-scale datasets. To address this scalability issue, we adopt an approximate k -NN graph construction method [25]. This approach builds on an extension of probabilistic skip-list-like structures to significantly reduce the computational cost, achieving a time complexity of $O(|N| \log |N|)$ and thus making it suitable for large data regimes.

6.3 Phase 3: Spectral Adversarial Robustness Evaluation

Let L_X and L_Y denote the Laplacian matrices of the original input graph and the k -NN graph constructed in the embedded feature space, respectively. Following the spectral robustness framework of [24], we make use of the leading eigenvalues of $L_Y^+ L_X$ and their corresponding eigenvectors to evaluate how sensitive each sample is to perturbations under a fixed model.

Concretely, we consider the generalized eigenvalue problem associated with $L_Y^+ L_X$ and build a weighted eigenspace matrix $V_s \in \mathbb{R}^{|V| \times s}$, which provides a spectral representation of the input manifold $G_X = (V, E_X)$, where $|V|$ is the number of nodes. The matrix V_s is defined as

$$V_s = [v_1 \sqrt{\zeta_1}, v_2 \sqrt{\zeta_2}, \dots, v_s \sqrt{\zeta_s}],$$

where $\zeta_1 \geq \zeta_2 \geq \dots \geq \zeta_s$ are the largest s eigenvalues of $L_Y^+ L_X$, and v_1, v_2, \dots, v_s are their associated eigenvectors.

Each node $p \in V$ is then mapped to the p -th row of V_s , yielding an s -dimensional spectral embedding. As described in [24], the robustness of an edge $(p, q) \in E_X$ can be characterized through the distance between the embeddings of its endpoints, measured as

$$\|V_s^\top e_{p,q}\|_2^2.$$

Based on this quantity, we define the *Spade score* of an edge (p, q) as

$$\text{Spade}(p, q) = \|V_s^\top e_{p,q}\|_2^2. \quad (2)$$

Edges with larger $\text{Spade}(p, q)$ values are interpreted as being less stable and more prone to perturbations along the directions encoded by their incident nodes.

6.4 Phase 4: Graph Pruning

For each edge in the original input graph, we rank the edges in decreasing order according to their Spade scores and select a proportion of the highest-scoring ones to form the set of non-robust edges. These edges are regarded as being most susceptible to noise and adversarial perturbations in both the graph structure and the feature space. We then remove this non-robust edge set from the original graph and adopt the resulting pruned graph as the new input for the GNN.

6.5 Experimental Results

We further evaluate robustness to global, structure-based attacks using a cumulative Nettack setting (Nettack-whole-test) on Cora. Starting from a clean graph, we sequentially apply Nettack to all test nodes that are initially classified correctly, accumulating all perturbations on a single shared adjacency matrix while keeping the GCN parameters fixed. On the original graph, the test accuracy drops sharply from 81.1% to 44.5%, and the attacked test nodes exhibit an attack success rate (ASR) of 45.37%. In contrast, on the Spade-pruned graph, the test accuracy only decreases from 79.9% to 72.5%, with a much lower ASR of 9.52%. These results indicate that, under a strong global adversary that perturbs the entire test set on a shared graph, Spade pruning substantially improves robustness by limiting the overall degradation in downstream performance.

7 Robust Spectral Clustering via Adversarial-Robustness-Guided Graph Pruning

Figure 3 shows the proposed method for pruning graphs for spectral clustering, which consists of five key phases: Phase (1) is initial graph construction. We build a k-NN graph from the input data; In Phase (2), we perform spectral embedding of the initial graph; In Phase (3), we construct a k-NN graph to

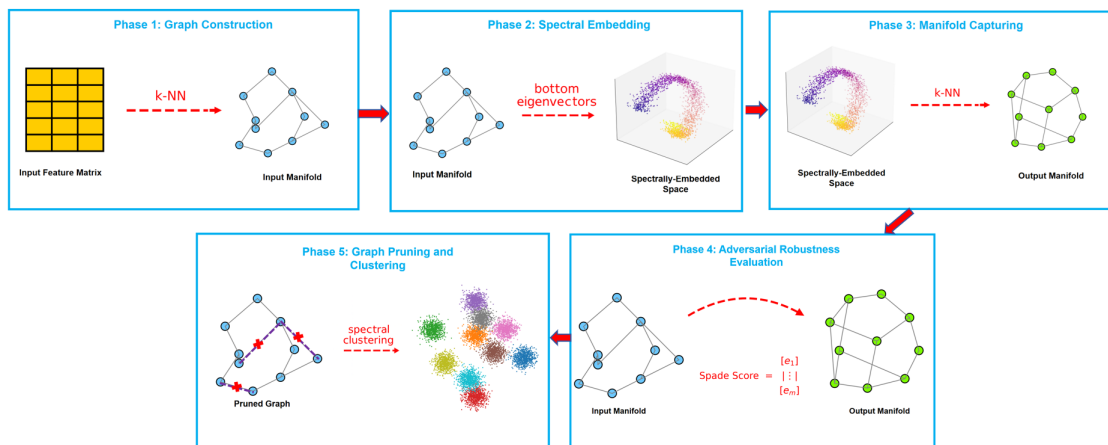


Fig. 3: Overview of the proposed method.

capture the manifold of the embedded space; In Phase (3), we calculate each edge’s level of non-robustness using the input graph and the output manifold; In Phase (5), we remove the top non-robust edges from the input graph and use it as the new input graph for spectral clustering.

The experimental results are shown in Table 4

Table 4: Clustering Accuracy (%)

Data Set	k -NN	Consensus	Spectral Spar	Robust Nodes	LSGL	Ours
COIL20	75.72	81.60	76.27	67.15	85.49	84.44
PenDigits	74.36	71.08	83.26	75.71	74.53	84.99
USPS	64.31	68.54	70.74	78.87	81.50	81.21
MNIST	59.68	61.09	60.09	70.40	-	68.21

8 Spectral Edge Attacks

We now introduce *Spectral Edge Attacks* (SEA), a family of adversarial structural perturbations guided by the Spade scores and the spectral embedding V_s . We assume a white-box adversary who has access to the trained GNN, the input graph, and the spectral quantities L_X, L_Y, V_s . Given a budget B on the number of undirected edge modifications, the goal is to select a set of edges to delete or add so as to maximally degrade the classification performance of the fixed GNN.

We consider two complementary variants: a *Spade-guided deletion attack*, which removes the most robust edges, and a *Spade-guided addition attack*, which inserts the most spectrally destabilizing edges.

8.1 Spade-Guided Edge Deletion Attack

Let $E_X^\uparrow = \{\{p, q\} : (p, q) \in E_X, p < q\}$ be the set of undirected edges in the original graph. We extend the Spade score in (2) to undirected edges by setting $\text{Spade}(\{p, q\}) = \text{Spade}(p, q)$ for any orientation.

Our first attack variant focuses on deleting edges that are most beneficial for the classifier. Spectrally, such edges are characterized by low Spade scores: their endpoints are close in the fragile spectral space, suggesting that they lie on the same local region of the manifold and that information propagation along these edges is stable. Removing them degrades the connectivity of the manifold and weakens the evidence supporting correct predictions.

Formally, we define the deletion score for each existing undirected edge as

$$S_{\text{del}}(\{p, q\}) = \text{Spade}(\{p, q\}). \quad (3)$$

Given a budget B , the Spade-guided deletion attack sorts all edges in ascending order of S_{del} and removes the top- B edges with the smallest scores. Let π_{del} be a permutation such that

$$S_{\text{del}}(\{p_{\pi_{\text{del}}(1)}, q_{\pi_{\text{del}}(1)}\}) \leq S_{\text{del}}(\{p_{\pi_{\text{del}}(2)}, q_{\pi_{\text{del}}(2)}\}) \leq \dots$$

Then the attack edge set is

$$\mathcal{E}_{\text{attack}}^{\text{del}} = \{\{p_{\pi_{\text{del}}(1)}, q_{\pi_{\text{del}}(1)}\}, \dots, \{p_{\pi_{\text{del}}(B)}, q_{\pi_{\text{del}}(B)}\}\}, \quad (4)$$

and the attacked graph is

$$\tilde{G}^{\text{del}} = (V, E_X \setminus \mathcal{E}_{\text{attack}}^{\text{del}}). \quad (5)$$

This deletion attack can be seen as the spectral dual of non-robust edge pruning: while pruning removes edges with large Spade scores to improve robustness, the deletion attack removes edges with small Spade scores to maximally disrupt the stable backbone of the manifold.

8.2 Spade-Guided Edge Addition Attack

Our second attack variant aims to *insert* edges between nodes whose spectral embeddings are most incompatible. Instead of modifying existing edges, the attacker considers candidate non-edges and uses the distance in the fragile spectral space to drive edge insertion.

Let $\bar{E}_X = \{\{p, q\} : p \neq q, \{p, q\} \notin E_X\}$ denote the set of undirected non-edges. For each $\{p, q\} \in \bar{E}_X$, we define a spectral incompatibility score

$$S_{\text{add}}(\{p, q\}) = \|V_s[p, :] - V_s[q, :]\|_2^2. \quad (6)$$

Intuitively, large values of S_{add} indicate that the two nodes are far apart along the most fragile spectral directions. Adding an edge between such nodes forces

the GNN to propagate messages along a path that conflicts with the underlying manifold, potentially distorting the representations and the decision boundary.

To further tailor the attack to the classifier, we also impose semantic constraints on candidate pairs. Let y_p be the true label and \hat{y}_p the predicted label of node p . Let \mathcal{T} be a set of target nodes, typically the subset of test nodes that are correctly classified, i.e., $\mathcal{T} = \{p \in V_{\text{test}} : \hat{y}_p = y_p\}$. We restrict candidate non-edges to those that satisfy

$$p \in \mathcal{T}, \quad y_p \neq y_q, \quad \{p, q\} \in \bar{E}_X, \quad (7)$$

so that adversarial edges connect nodes from different classes and only attack nodes that the model currently handles correctly.

The Spade-guided addition attack then proceeds in two stages:

1. For each target node $p \in \mathcal{T}$, we enumerate or sample a subset of candidate neighbors q that satisfy the above constraints, compute $S_{\text{add}}(\{p, q\})$, and retain the top-scoring candidate for each p .
2. We pool all these candidate edges into a global list, sort them in descending order of S_{add} , and select the top- B pairs as adversarial edges:

$$\mathcal{E}_{\text{attack}}^{\text{add}} = \arg \max_{\mathcal{E} \subseteq \bar{E}_X, |\mathcal{E}|=B} \sum_{\{p, q\} \in \mathcal{E}} S_{\text{add}}(\{p, q\}). \quad (8)$$

The attacked graph is obtained by inserting these edges:

$$\tilde{G}^{\text{add}} = (V, E_X \cup \mathcal{E}_{\text{attack}}^{\text{add}}). \quad (9)$$

In practice, to avoid quadratic enumeration over all non-edges, we can approximate the candidate set by using a k' -nearest neighbor search in the spectral space V_s , but selecting the *farthest* neighbors among those with different labels. This yields an efficient and scalable approximation of the ideal Spade-guided addition attack.

9 Conclusion

This work introduces a novel method for training Graph Neural Networks (GNNs) by utilizing the top non-robust training samples from the training set. First, we embed the data using a GNN to obtain feature representations, followed by the construction of k -nearest neighbor (k -NN) graphs to capture the underlying data manifolds of both the input and embedded feature matrices. In the third phase, we assess each node’s robustness using spectral adversarial robustness evaluation, which quantifies their susceptibility to noise. Finally, we enhance the GNN’s robustness by training it exclusively on the small training set composed of the non-robust samples identified from the training set. Experimental results demonstrate that our method significantly improves the training of the three most popular GNN models on three widely-used benchmark datasets. We also proposed a robust-node based hypergraph partitioning method, an adversarial robustness based graph pruning method for GNN defenses, spectral clustering and a related spectral edge attack method. Experiments also demonstrated their effectiveness.

References

1. T. N. Kipf and M. Welling, “Semi-supervised classification with graph convolutional networks,” *arXiv preprint arXiv:1609.02907*, 2016.
2. P. Veličković, G. Cucurull, A. Casanova, A. Romero, P. Lio, and Y. Bengio, “Graph attention networks,” *arXiv preprint arXiv:1710.10903*, 2017.
3. Z. Hu, Y. Dong, K. Wang, K.-W. Chang, and Y. Sun, “Gpt-gnn: Generative pre-training of graph neural networks,” in *Proceedings of the 26th ACM SIGKDD international conference on knowledge discovery & data mining*, 2020, pp. 1857–1867.
4. J. Zhou, G. Cui, S. Hu, Z. Zhang, C. Yang, Z. Liu, L. Wang, C. Li, and M. Sun, “Graph neural networks: A review of methods and applications,” *AI open*, vol. 1, pp. 57–81, 2020.
5. W. Fan, Y. Ma, Q. Li, Y. He, E. Zhao, J. Tang, and D. Yin, “Graph neural networks for social recommendation,” in *The world wide web conference*, 2019, pp. 417–426.
6. B. Yu, H. Yin, and Z. Zhu, “Spatio-temporal graph convolutional networks: A deep learning framework for traffic forecasting,” *arXiv preprint arXiv:1709.04875*, 2017.
7. A. Mirhoseini, A. Goldie, M. Yazgan, J. W. Jiang, E. Songhori, S. Wang, Y.-J. Lee, E. Johnson, O. Pathak, A. Nazi *et al.*, “A graph placement methodology for fast chip design,” *Nature*, vol. 594, no. 7862, pp. 207–212, 2021.
8. M. Song, Z. Zhan, and E. Haihong, “Hierarchical schema representation for text-to-sql parsing with decomposing decoding,” *IEEE Access*, vol. 7, pp. 103 706–103 715, 2019.
9. R. Ying, R. He, K. Chen, P. Eksombatchai, W. L. Hamilton, and J. Leskovec, “Graph convolutional neural networks for web-scale recommender systems,” in *Proceedings of the 24th ACM SIGKDD international conference on knowledge discovery & data mining*, 2018, pp. 974–983.
10. I. Goodfellow, P. McDaniel, and N. Papernot, “Making machine learning robust against adversarial inputs,” *Communications of the ACM*, vol. 61, no. 7, pp. 56–66, 2018.
11. A. Fawzi, O. Fawzi, and P. Frossard, “Analysis of classifiers’ robustness to adversarial perturbations,” *Machine learning*, vol. 107, no. 3, pp. 481–508, 2018.
12. D. Zügner, A. Akbarnejad, and S. Günnemann, “Adversarial attacks on neural networks for graph data,” in *Proceedings of the 24th ACM SIGKDD international conference on knowledge discovery & data mining*, 2018, pp. 2847–2856.
13. K. Xu, H. Chen, S. Liu, P.-Y. Chen, T.-W. Weng, M. Hong, and X. Lin, “Topology attack and defense for graph neural networks: An optimization perspective,” *arXiv preprint arXiv:1906.04214*, 2019.
14. R. Feinman, R. R. Curtin, S. Shintre, and A. B. Gardner, “Detecting adversarial samples from artifacts,” *arXiv preprint arXiv:1703.00410*, 2017.
15. J. H. Metzen, T. Genewein, V. Fischer, and B. Bischoff, “On detecting adversarial perturbations,” *arXiv preprint arXiv:1702.04267*, 2017.
16. P. Yang, J. Chen, C.-J. Hsieh, J.-L. Wang, and M. Jordan, “MI-loo: Detecting adversarial examples with feature attribution,” in *Proceedings of the AAAI Conference on Artificial Intelligence*, vol. 34, no. 04, 2020, pp. 6639–6647.
17. C. Agarwal, A. Nguyen, and D. Schonfeld, “Improving robustness to adversarial examples by encouraging discriminative features,” in *2019 IEEE International Conference on Image Processing (ICIP)*. IEEE, 2019, pp. 3801–3505.
18. X. Liu, Y. Li, C. Wu, and C.-J. Hsieh, “Adv-bnn: Improved adversarial defense through robust bayesian neural network,” *arXiv preprint arXiv:1810.01279*, 2018.

19. W. Hamilton, Z. Ying, and J. Leskovec, "Inductive representation learning on large graphs," *Advances in neural information processing systems*, vol. 30, 2017.
20. F. R. Chung, *Spectral graph theory*. American Mathematical Soc., 1997, vol. 92.
21. U. Von Luxburg, "A tutorial on spectral clustering," *Statistics and computing*, vol. 17, pp. 395–416, 2007.
22. G. H. Golub and C. F. Van Loan, *Matrix computations*. JHU press, 2013.
23. K. Sharma, S. Verma, S. Medya, A. Bhattacharya, and S. Ranu, "Task and model agnostic adversarial attack on graph neural networks," in *Proceedings of the AAAI Conference on Artificial Intelligence*, vol. 37, no. 12, 2023, pp. 15 091–15 099.
24. W. Cheng, C. Deng, Z. Zhao, Y. Cai, Z. Zhang, and Z. Feng, "Spade: A spectral method for black-box adversarial robustness evaluation," in *International Conference on Machine Learning*. PMLR, 2021, pp. 1814–1824.
25. Y. A. Malkov and D. A. Yashunin, "Efficient and robust approximate nearest neighbor search using hierarchical navigable small world graphs," *IEEE transactions on pattern analysis and machine intelligence*, vol. 42, no. 4, pp. 824–836, 2018.